1989

A New Narrow-Line Seyfert 1 Galaxy: IRAS 1652+395

L. Bassani

M. J. Coe

M. A. Malkan

Bruce Partridge
Haverford College, bpartrid@haverford.edu

Repository Citation
(with Bassani and others) A New Narrow-Line Seyfert 1 Galaxy: IRAS 1652+395, Ap. J., 344, 726, 1989.

1989

A New Narrow-Line Seyfert 1 Galaxy: IRAS 1652+395

L. Bassani

M. J. Coe

M. A. Malkan

R. Bruce Partridge
Haverford College

THE ASTROPHYSICAL JOURNAL, 344:726–733, 1989 September 15

A NEW NARROW-LINE SEYFERT 1 GALAXY: IRAS 1652+395

L. BASSANI,[1] M. J. COE,[2] M. A. MALKAN,[3] N. MANDOLESI,[4] B. PARTRIDGE,[4] AND L. SPINOGLIO[3,5]

Received 1988 December 9; accepted 1989 February 28

ABSTRACT

Multiwavelength observations—from radio to X-rays—of IRAS 1652+395, a far-infrared and X-ray source serendipitously discovered in the field of the BL Lac object Mrk 501, are reported. They show that IRAS 1652+395 is a new Seyfert 1 galaxy at a redshift of $z = 0.069$. The Balmer emission lines are only slightly broader (~ 1000 km s^{-1} FWHM) than the forbidden lines, suggesting a classification as a narrow-line Seyfert 1 galaxy, as reported by Osterbrock and Pogge in 1985. Its energy distribution from far-IR to X-ray frequencies is well fitted by starlight plus a power law of spectral index $\alpha = -1.2$, with no evidence of a "blue bump." The object is the first active galaxy to be identified through both its far-infrared and X-ray emission.

Subject headings: galaxies: individual (IRAS 1652+395) — galaxies: redshifts — galaxies: Seyfert — galaxies: X-rays — infrared: sources

I. INTRODUCTION

IRAS Guest observations made in the deep sky photometric mode detected a serendipitous source, IRAS 1652+395, 20′ south of the target, the BL Lac object Mrk 501. Preliminary results of two pointed *IRAS* observations and of 6 cm VLA observations have been reported by Bassani *et al.* (1986), in a search for radio counterparts of serendipitous *IRAS* sources. Analysis of *Einstein* and *EXOSAT* soft X-ray data of the same field revealed a source located only 38″ from IRAS 1652+395 (Bassani *et al.* 1987*b*).

Although no identification was found in existing astronomical catalogs, the possible coincidence of the far-infrared and soft X-ray source at high Galactic latitude ($b > 50°$), and the shape of the far-infrared energy distribution led us to suggest its extragalactic nature (Bassani *et al.* 1986).

To test this hypothesis, we analysed and co-added all the best available *IRAS* pointed observations and observed the region within the *IRAS* error box at various wavelengths. Once a plausible optical counterpart, a new narrow-line Seyfert 1 galaxy, was found, we obtained detailed follow-up observations. In this paper we present all the data so far collected on this serendipitous source.

II. OBSERVATIONS

a) IRAS Data

In addition to the all-sky survey, the *Infrared Astronomical Satellite* (*IRAS*) made pointed observations of preselected targets for better sensitivity than the Point Source Catalogue. Raster scans were made of a region 0°.5 × 1°.5 centered on the target source.

To improve on the *IRAS* fluxes of IRAS 1652+395 given by Bassani *et al.* (1986), all the 20 available pointed observations of the region containing Mrk 501 were examined at the *IRAS* database at Rutherford Appleton Laboratories. Each single observation took about 600 s of observing time and resulted in a signal-to-noise ratio gain of 6–8 over the Point Source Catalogue. The data were analysed using IPMAF (*IRAS* Post Mission Analysis Facility at Rutherford Appleton Laboratories, U.K.) and calibrated using the 1984 June *IRAS* absolute calibration. This incorporates a correction for the nonlinear resistor. The calibration is probably accurate to 5% at 12 and 25 μm and 10% at 60 and 100 μm. No color correction factor has been applied to the flux densities, which is equivalent to assuming $S(\nu) \propto \nu^{-1}$, where $S(\nu)$ is the flux at ν. Flux densities and positions were then evaluated by co-adding overlapping grids to obtain the best available signal-to-noise ratio. The eight best S/N images were used for the final result, with there being no evidence for variability between images. The resulting *IRAS* photometry is given in Table 1; the flux densities and 1 σ errors are in mJy. We quote the 100 μm flux only as an upper limit due to contamination from extended cirrus emission.

We obtained the best source position from a weighted average of the 12, 25, and 60 μm positions, which is, for epoch 1950,

$$\text{R.A.} = 16^h52^m25^s.1 \pm 6^s.5, \quad \text{decl.} = 39°30'39''.9 \pm 48''.7$$

where the uncertainty corresponds to the FWHM or 2.35 σ error box.

b) X-Ray Data

X-ray observations of the *IRAS* field or part of it were obtained from the data banks of both the *Einstein* and *EXOSAT* satellites (Bassini *et al.* 1987*b*). The *Einstein* data were taken with the IPC (Imaging Proportional Counter) instrument two times in 1980. The *EXOSAT* observations were made at several epochs during 1984 with only one Low Energy (LE) telescope operating in the imaging mode with the CMA (Channel Multiplier Array) in the focal plane. Both instruments operate at soft X-ray energies but are sensitive to slightly different energy bands (0.05–2.0 keV for the LE/CMA and 0.3–3.5 keV for the IPC). In particular, the CMA has been used with 3 different filters (aluminum/Parylene, Thin Lexan, and boron) in each measurement, thus providing a modest degree of energy discrimination. Details of the X-ray data analysis can be found in Bassani *et al.* (1987*a*).

A source was detected in both *Einstein* measurements but only in three *EXOSAT* observations out of a total of eight analyzed. The object was found on exposures taken with the

[1] Istituto TE.S.R.E.-C.N.R., Bologna.
[2] Physics Department., Southampton University.
[3] Astronomy Department, University of California, Los Angeles.
[4] Astronomy Department, Haverford College.
[5] Istituto F.S.I.-C.N.R., Frascati.

TABLE 1

MULTIFREQUENCY OBSERVATIONS OF IRAS 1652+395

Energy Range: Wavelength	Instrument	Date	Fluxes (mJy)	Comments
Radio:				
6 cm	VLA	1985 Sept 10	<0.4	5 σ upper limit
20 cm	VLA	1986 Oct 23	<2.5	5 σ upper limit
Far-infrared:				
100 μm	*IRAS*	1983 Aug–Oct	<195	3 σ upper limit
60 μm	*IRAS*	1983 Aug–Oct	98.1 ± 7.2	
25 μm	*IRAS*	1983 Aug–Oct	36.8 ± 5.2	
12 μm	*IRAS*	1983 Aug–Oct	17.9 ± 4.6	
Near-infrared:				
J	UKIRT	1988 Mar 22	3.20 ± 020	IRCAM
H	UKIRT	1988 Mar 22	3.30 ± 0.20	IRCAM
K	UKIRT	1988 Mar 22	3.50 ± 0.10	IRCAM
J	UKIRT	1987 Apr 10	3.03 ± 0.06	Aperture 12″.4
H	UKIRT	1987 Apr 10	3.71 ± 0.15	Aperture 12″.4
K	UKIRT	1987 Apr 10	3.70 ± 0.07	Aperture 12″.4
L′	UKIRT	1987 Apr 10	5.59 ± 1.50	Aperture 12″.4
J	TIRGO	1987 May 8/10	3.15 ± 0.23	Aperture 17″
H	TIRGO	1987 May 8/10	3.55 ± 0.13	Aperture 17″
K	TIRGO	1987 May 8/10	3.45 ± 0.32	Aperture 17″
Optical:				
Hα	Lick	1987 July–Aug	7.0×10^{-14}	ergs cm^{-2} s^{-1}
Hβ	Lick	1987 July–Aug	1.9×10^{-14}	ergs cm^{-2} s^{-1}
[O III]5007	Lick	1987 July–Aug	1.1×10^{-14}	ergs cm^{-2} s^{-1}
4520 Å	Lick	1987 July–Aug	0.55	Continuum bins
4750 Å	Lick	1987 July–Aug	0.58	Continuum bins
5045 Å	Lick	1987 July–Aug	0.64	Continuum bins
5420 Å	Lick	1987 July–Aug	0.70	Continuum bins
5800 Å	Lick	1987 July–Aug	0.90	Continuum bins
5900 Å	Lick	1987 July–Aug	0.87	Continuum bins
5980 Å	Lick	1987 July–Aug	0.88	Continuum bins
6060 Å	Lick	1987 July–Aug	0.90	Continuum bins
6150 Å	Lick	1987 July–Aug	0.98	Continuum bins
6450 Å	Lick	1987 July–Aug	1.02	Continuum bins
6560 Å	Lick	1987 July–Aug	1.04	Continuum bins
6650 Å	Lick	1987 July–Aug	1.04	Continuum bins
7260 Å	Lick	1987 July–Aug	1.10	Continuum bins
7380 Å	Lick	1987 July–Aug	1.28	Continuum bins
7740 Å	Lick	1987 July–Aug	1.29	Continuum bins
7920 Å	Lick	1987 July–Aug	1.26	Continuum bins
Ultraviolet:				
1250–1950 Å	*IUE*	1987 Feb 20	6.5 ± 11.6	
X-ray:				
0.3–3.5 keV	*Einstein*	1980 Jan–Aug	$(0.26 \pm 0.03) \times 10^{-3}$	Assume energy index $\alpha = -0.5$ and $N_H = 3 \times 10^{20}$ cm^{-2}
0.05–2 keV	*EXOSAT*	1984 Feb 2–6	$(1.42 \pm 0.23) \times 10^{-3}$	Assume energy index $\alpha = -0.5$ and $N_H = 3 \times 10^{20}$ cm^{-2}

Thin Lexan and aluminum/Parylene filters but not with the boron (highest energy) filter. In order to obtain the best source position, we have summed all *EXOSAT* filter images rotated to the same roll angle and determined the position of the peak emission, which is

$$\text{R.A.} = 16^h52^m27^s.9, \text{ decl.} = 39°30'20''.2$$

with an uncertainty of ±20″. The *EXOSAT* position is offset from the *Einstein* position by 24″; however, the *EXOSAT* error box lies well within the much larger *Einstein* error box (Fig. 1), so we conclude that both telescopes detected the same X-ray object.

The finding chart from the POSS (Palomar Observatory National Geographic Society Sky Survey) red plate of the field around IRAS 1652+395 is shown in Figure 1 together with the FWHM error boxes relative to the *IRAS*, *Einstein*, and *EXOSAT* satellites. It is evident that the *EXOSAT* observation, by reducing the uncertainty in the X-ray position, allows the identification of the soft X-ray source with object 3. Furthermore the optical spectrum of object 3 is typical of active galaxies (see § II*d* for details), which are strong far-IR and X-ray emitters, while objects 1 and 2 have optical spectra of normal stars. We therefore identify the *IRAS*/X-ray source with the active galaxy.

The X-ray fluxes given in Table 1 are obtained assuming a "standard" power law of energy index $\alpha = -0.5$ and a local column density $N_H = 3 \times 10^{20}$ cm^{-2}, which is a lower limit to the amount of hydrogen measured by Heiles (1975) in the general direction of the source. Under these assumptions, it is possible to reduce the data to approximately the same X-ray energy band in order to compare them. It is clear from Figure 2 that the source flux decreased by a factor of about 7 from one set of satellite observations to the other, while no significant evidence for variability is present within each individual set of data. Seyfert galaxies are known to vary in X-rays by factors of up to ~10 over long time scales of years; the possibility that our source is variable in this band makes an additional observation very desirable.

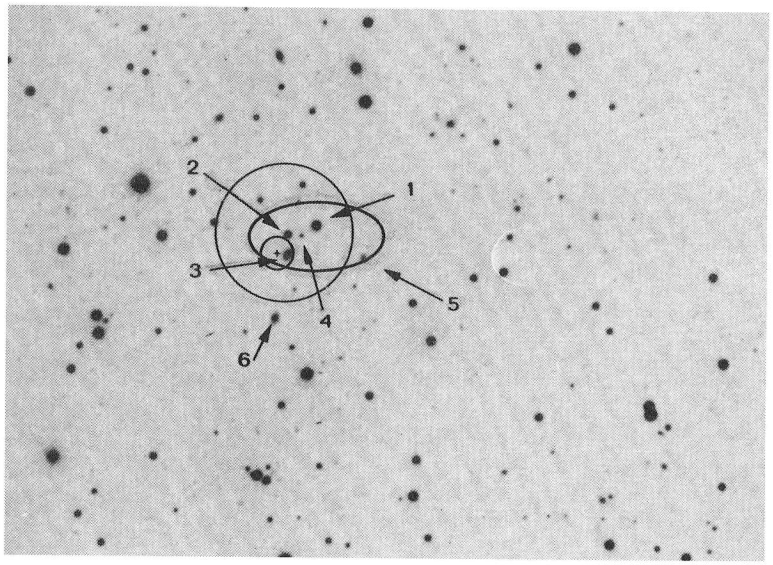

FIG. 1.—Finding chart from the Palomar survey (red plate) for IRAS 1652+395, showing the 2.35 σ error boxes relative to the *IRAS* (*ellipse*), *Einstein* (*large circle*), and *EXOSAT* (*small circle*) satellites. Object 3 is the counterpart of the infrared/X-ray source. Positions for all objects in the figure can be found in Table 2.

On the other hand, if no assumption is made on the spectrum and the source is assumed not to vary, it is possible to constrain the spectral parameters by the ratio of the CMA to the IPC count rates ($\sim$0.3). The observed value constrains the energy index to be < -2.5 if $N_H > 3 \times 10^{20}$ cm^{-2} (Bassani *et al.* 1987*a*). Such a soft spectrum would also be consistent with the comparison of the counts rates measured with the Thin Lexan and aluminum/Parylene filters. This object adds to the growing number of AGNs which have been found recently to have steep power law spectra below 1–2 keV (energy slopes range from -1.5 to -4; Bedford, Vilhu, and Petrov 1988 and references therein).

c) Radio Data

Radio observations of the field containing the *IRAS* source were made with the VLA using 100 and 50 MHz effective band widths centered on 4860 MHz ($\sim$6 cm) and 1450 MHz ($\sim$20 cm), respectively. A description of the instrument is given by Thompson *et al.* (1980).

The array was in "C" configuration with 25 antennas operating, and the field was mapped in one or two 30 minute exposures at each wavelength. Both measurements (6 and 20 cm) were repeated after an interval of about 1 year, but there was no difference between the two sets of data. The radio maps were reduced and cleaned with standard NRAO procedures. They reveal a source within the *IRAS* error box, object 5 in Figure 1 and Table 2, at the position given in Table 2 with an associated uncertainty of $\pm 6''$. Its total flux densities are 4.5 and 10 mJy at 6 and 20 cm, respectively, after correction for primary beam attenuation. Two other weaker sources were present in the 6 cm map but outside the *IRAS* error ellipse.

Although a physical association of the most intense VLA

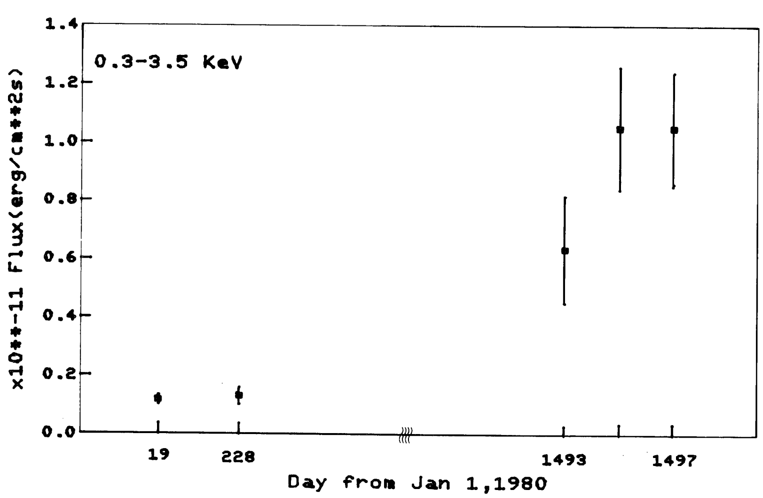

FIG. 2.—Long-term X-ray light curve of IRAS 1652+395 as measured by *EXOSAT* and *Einstein* under the assumption of a "standard" power law of energy index $\alpha = -0.5$ and column density $N_H = 3 \times 10^{20}$ cm^{-2}.

TABLE 2

CCD AND VLA OBJECTS

Object	R.A.(1950)	Decl.(1950)	*i* Magnitude	Comments
1...........	16^h52^m24^s.57	39°30′48″.1	15.6	CCD object
2...........	16 52 27.02	39 30 39.9	16.5	CCD object
3...........	16 52 27.02	39 30 20.4	16.7	CCD object
4...........	16 52 25.81	39 30 38.3	18.3	CCD object
5...........	16 52 20.5	39 30 17.2	...	VLA object
6...........	16 52 27.6	39 29 18.6	17.85	CCD object

source with the far-infrared object is possible given the large uncertainties in the *IRAS* position, it appears unlikely given the considerations presented below (see § III for details). Therefore, we also estimated the 5 σ upper limits at 6 and 20 cm in the position of the *IRAS* source as reported in Table 1. IRAS 1652+395 is displaced from object 3, the most likely counterpart, by about 30″ and from the VLA source by about 58″. A physical association of the *IRAS* object with the VLA source or with one of the other three objects contained within the *IRAS* error box, while not completely ruled out, appears, however, unlikely both because of the differences in position and the spectroscopic results.

d) *Optical Data*

Optical CCD images of the field around the *IRAS* error ellipse have been obtained at the 3.0 m Shane telescope of Lick Observatory in the *i* band. The CCD processing was standard. Four objects were clearly visible both in the CCD images and in an enlargement of the POSS red plate of the same sky region (Fig. 1): three apparently stellar objects (hereafter objects 1, 2, and 4) and one galaxy (object 3), at the positions listed in Table 2. A fifth object to the south was also visible on the Lick images. It is a galaxy also listed in Table 2, as object 6. The associated positional errors are 0″.4 and 0″.5 in R.A. and decl., respectively.

Two consecutive far-red images obtained at Lick gave reasonably consistent magnitude estimates, and these are also listed in Table 2. The Wratten 9 filter and CCD long-wavelength cutoff defined an effective wavelength of roughly 8000 Å for these observations. Since they were made in the presence of some cirrus, the relative magnitudes are more accurate than the absolute values (which could be systematically out by 30%).

The four objects near the *IRAS* position were spectroscopically observed with the Isaac Newton telescope (INT, Canary islands) on 1987 February 21; only one (object 4) was too faint to be detectable. The total exposure time was 2200 s using the Intermediate Dispersion Spectrograph (IDS) and the Imaging Photon Counting System (IPCS). The arcminute-long slit allowed two objects to be measured at once, with a resolution of 2–3 Å over the wavelength range 4000–7300 Å. Of the three objects detected, two had normal stellar spectra, while object 3 was clearly an emission line object.

This result has been confirmed by subsequent observations of object 3 with the Lick 1.0 m Nickel telescope on 1987 July 13 and 15 and the 3.0 m telescope on 1987 August 31, using the CCD transmission grating spectrographs (Lauer *et al.* 1984) at the Cassegrain foci of both telescopes. The spectra were obtained with slit widths of 8″.8 and 3″.9, with 600 lines mm^{-1} and 420 lines mm^{-1} grisms at resolutions of ~8 and ~5 Å per pixel, respectively, both covering a wavelength range of ~4500–8500 Å. The optical spectra were flux-calibrated with repeated measurements of spectroscopic standard stars (Stone 1974, 1977), and wavelength-calibrated using emission lines of He, Ne, Hg, and Cd from standard comparison lamps and sky lines of Na I, measured simultaneously with the celestial objects.

The CCD images indicate that the 8″.8 slit included at least 95% of the far-red light of the galaxy. The 3″.9 slit included $\frac{2}{3}$ of the total light, and this estimate agrees with the ratio of 8000 Å fluxes measured with the two slits.

Figure 3 shows a flux-calibrated optical spectrum of object

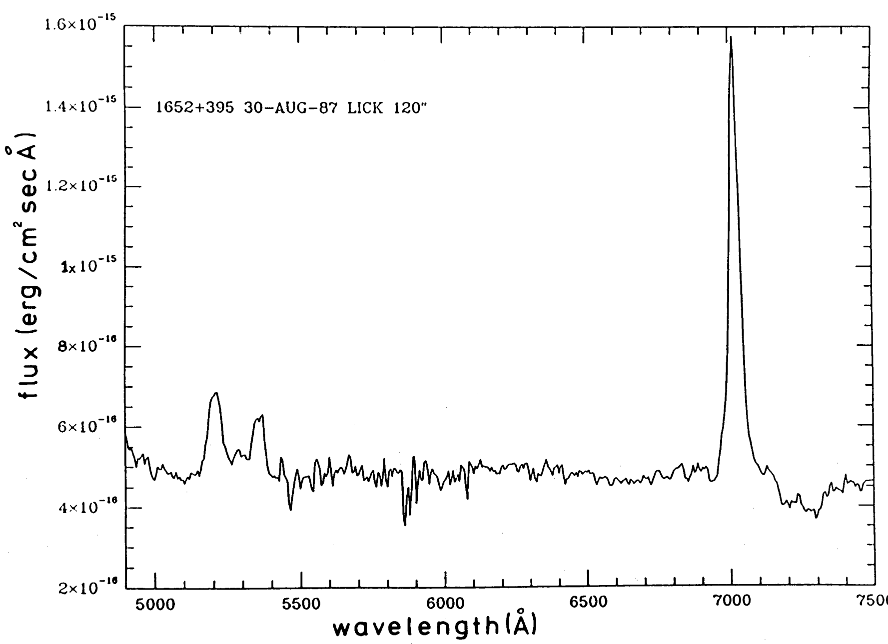

FIG. 3.—Flux calibrated optical spectrum of IRAS 1652+395 (object 3 in Fig. 1) taken with the Lick 3 m telescope. The redshift derived from the Balmer lines is $z = 0.069$.

3. It has strong Balmer and [O III] 5007, 4959 emission lines. The heliocentric redshift derived from the first three Balmer lines is $z = 0.0689 \pm 0.0001$, corresponding to a distance of 413 Mpc (assuming $H_0 = 50$ km s^{-1} Mpc^{-1} for the Hubble constant).

We believe the flux determination of the 3 m spectrum is good since it yields the same integrated Hα flux (7×10^{-14} ergs cm^{-2} s^{-1}) as the 1 m spectra. As expected, the broad emission line flux is entirely concentrated on the nucleus, unlike the stellar continuum.

e) Near-Infrared Data

Once the most obvious optical counterpart to the far-IR and X-ray source was found, i.e., the emission-line source (object 3), near-infrared photometric observations were made. *J, H, K, L′* photometry was obtained at the UKIRT 3.8 m telescope (Mauna Kea, Hawaii) on 1987 April 10, through a 12″.4 aperture. *JHK* photometry has also been collected at the 1.5 m TIRGO telescope (Gornergrat, Switzerland) with a 17″ aperture. InSb detectors with standard filters were used at both telescopes, and the data were calibrated relative to sets of standard stars measured throughout the nights.

The infrared camera, IRCAM on the UKIRT (McLean *et al.* 1986), has also been used to observe 1652+395 on 1988 March 22. Each of the 62 × 58 pixels was 1″.2 on a side. Exposures of 300 s were made in each of the three wavebands *J*, *H*, and *K*. Flat-fields were also obtained as were calibration observations of HD 161903 and "dark" exposures. The images were analyzed by first extracting the appropriate dark currents and then dividing by the flat fields. Fluxes were determined by setting software apertures on the image around the target or the calibration star and then subtracting the background from a similar-sized adjacent area. There is no significant difference among the three sets of observations, an indication of the constancy of the flux at these wavelengths.

f) Ultraviolet Data

An ultraviolet spectrum of object 3 was obtained with the *IUE* satellite over the wavelength range 1250–1950 Å using the short-wavelength camera (image SWP 30345) in the low-dispersion mode (effective resolution < 10 Å). The source was observed in a large-aperture (10″ × 20″) exposure of 180 minutes. To ensure continuity between the optical and ultraviolet spectra, the *IUE* observation was scheduled within a day of the optical spectroscopy at the INT telescope. Unfortunately, the source was too faint to be detected, so only an upper limit was obtained.

III. RESULTS

a) Emission Lines

The [O III] 5007/Hβ intensity ratio of ~0.55 and the Balmer decrement Hα/Hβ ~3.7 are typical of Seyfert 1's (Osterbrock 1977). Permitted Fe II emission lines may be present, but they are quite weak. The Hα and Hβ full widths at half-maximum are 1000 km s^{-1}. The Hα profile of the source obtained from INT is shown in Figure 4; the full width at zero intensity corresponds to 4400 km s^{-1}. In the left wing of the Hα line, a blend with [N II] 6548 is evident. The permitted Balmer lines are not dramatically broader than the forbidden [O III] 5007 line, which has a FWHM of 500 km s^{-1}, suggesting that IRAS 1265+395 is more accurately classified as a "narrow-line Seyfert 1 galaxy" (Osterbrock and Pogge 1985).

Other than the aperture effects attributed to starlight, we found no evidence of optical continuum or line variations throughout the summer of 1987.

b) Starlight

Figure 1 shows that 1652+395 resides in the nucleus of a small, apparently flattened galaxy. It is probably a spiral viewed at fairly high inclination. The growth curve of total counts versus aperture diameter from the CCD images show

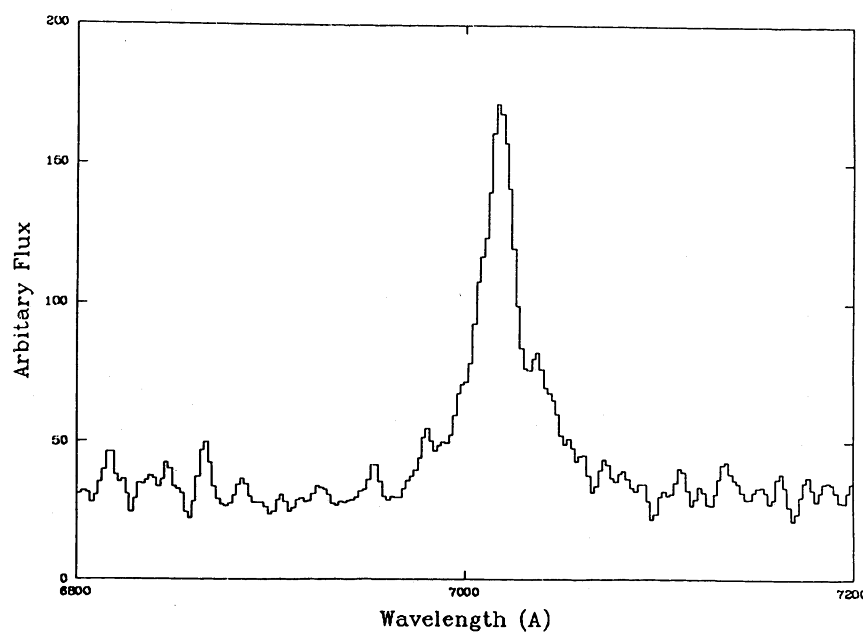

FIG. 4.—The Hα profile of the source obtained with the Isaac Newton telescope. The full width at zero intensity corresponds to 4400 km s^{-1}.

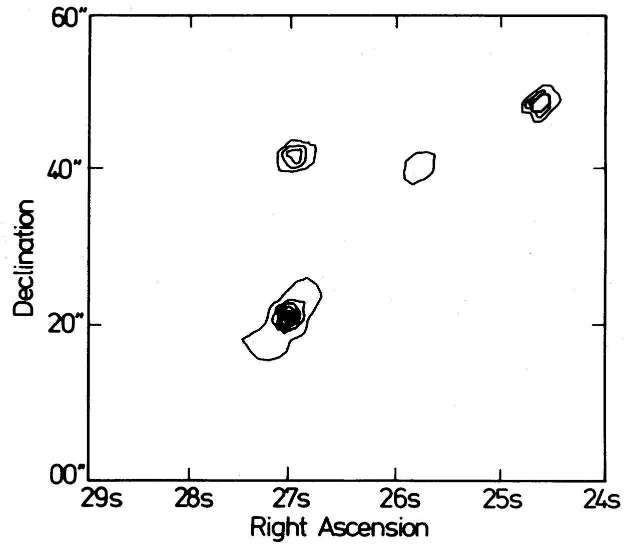

FIG. 5.—An infrared image in the K band of the region surrounding 1652+395. The coordinates at 1950 are $+16^h52^m$ in right ascension and $+30°30'$ in declination. The image has been enhanced using maximum entropy.

that virtually all of the galaxy flux is included within a radius of 8″.

The near-infrared colors of the source ($J-H=0.73$, $H-K=0.56$) are typical of Seyfert galaxies with significant contributions from starlight. The K band image (Fig. 5) shows the faint NW–SE elongation of the galaxy surrounding the active nucleus. At most 15%–20% of the total K flux falls outside of the central 5″. This estimate is consistent with our CCD image measurement that 30% of the i flux falls outside of the central 5″, given the fact that the nucleus has a redder $[i-K]$ color than starlight.

Two stellar absorption features (Mg I b 5175 and Na I D 5893) may be detected in the 3 m (3″.9 slit) spectrum. However, they are very weak, with equivalent widths of only 1 or 2 Å, and are hardly stronger than many noise features. The weakness of these absorptions is consistent with our estimate that the nuclear spectrum is predominantly nonstellar.

c) *Nonstellar Continuum*

The warm/blue 60 to 25 μm infrared color of IRAS 1652+395 [$\alpha(25, 60\ \mu m) = -1.1 \pm 0.2$] is typical of an active galaxy (de Grijp *et al.* 1985) and therefore consistent with the Seyfert nature of the optical spectrum. Miley, Neugebauer and Soifer (1985) examined the distribution in luminosity of the Seyfert galaxies (their Fig. 2). Adopting their definition $L = \nu L\nu$, we obtain $L(60\ \mu m) = 1.0 \times 10^{44}$ ergs s^{-1} (or $2.6 \times 10^{10}\ L_\odot$), which places our object among the most luminous 25% of *IRAS* type 1 Seyferts. The luminosity in other wavebands is comparable to the far-infrared luminosity.

It is not surprising that the galaxy was not detected at radio wavelengths: de Jong *et al.* (1985) have found that the far-infrared [S_{ir}(60 μm)] and radio [S_r(6.3 cm)] flux densities of a large sample of spiral galaxies, including active ones, are closely correlated by $\log S_r = (0.94 \pm -0.06) \log S_{ir} - (2.34 \pm -0.06)$ (flux densities in Jy). For the observed value of S_{ir} we estimated a 6 cm flux of 0.5 ± 0.2 mJy, consistent with the 5 σ upper limit imposed by the VLA observations.

We used the scheme of Edelson, Malkan, and Rieke (1987) to further classify the continuum emission of IRAS 1652+395. From their analysis of a complete sample of Seyfert galaxies, they proposed, using the (2.2–25 μm)/(12–60 μm) color-color diagram, to discriminate between flat power-law spectra (typical of the nonthermal emission of Seyfert 1's and quasars), and steep curved spectra (typical of the thermal dust emission of Seyfert 2's). The spectral indices of IRAS 1652+395, computed using the UKIRT 2.2 μm flux in the 12″.4 aperture, are $\alpha(2.2\text{–}25\ \mu m) = -0.95$ and $\alpha(12\text{–}60\ \mu m) = -1.06$, which place this object among the Seyfert 1's and optically selected quasars, in a region which completely excludes Seyfert 2's. Another test of the nonthermal nature of IRAS 1652+395 can be made using the 2 keV and 3.5 μm flux densities. Taking the *Einstein* 2 keV flux and the UKIRT photometry in the 12″.4 aperture (Table 1), the derived infrared–to–X-ray slope is −1.15, again consistent with the mean value of -1.18 ± 0.02 derived for an heterogeneous sample of Seyfert 1's and quasars (Malkan and Sargent 1982; Malkan 1985; Edelson and Malkan 1986). This infrared–to–X-ray ratio is quite typical of AGNs which have been discovered by means of their X-ray emission (Reichert *et al.* 1982; Kriss and Canizares 1982; Margon, Chanan, and Downes 1982).

The amount of internal reddening of the active nucleus also appears to be correlated with the slope of the continuum (Edelson and Malkan 1986). Unfortunately the failure to detect the source at UV wavelengths prevents us from accurately estimating the reddening. Although not completely reliable because of radiative transfer effects, the Balmer decrement may give a rough estimate of the extinction in the nucleus. If we compare the observed ratio of $H\alpha/H\beta = 3.7$ with the "case B" value of 3.1 for photoionization by a power law (Gaskell and Ferland 1984), we obtain a crude upper limit to the total extinction of $E(B-V) \sim 0.3$. Since the reddening due to the line-of-sight dust in the Milky Way is only $E(B-V) \sim 0.08$ (Burstein and Heiles 1978), an upper limit to the internal reddening might be $E(B-V) \sim 0.2$.

To further investigate this question, we used Ward *et al.*'s classification (1987) of Seyfert type 1's as "bare" AGNs (class A), reddened AGNs (class B), and "galaxy-dominated" AGNs (class C). Using their reddening index $\log [\nu F\nu(1.2\ \mu m)/\nu F\nu(0.36\ \mu m)] = 0.4$ versus cool dust far-infrared index $\log [\nu F\nu(60\ \mu m)/\nu F\nu(12\ \mu m)] = 0.04$ or versus near-infrared slope $\log [\nu F\nu(3.5\ \mu m)/\nu F\nu(1.2\ \mu m)] = 0.4$, IRAS 1652+395 can be classified as a class B/class C borderline object, i.e., as a moderately reddened AGN, but with some contamination from the underlying galaxy, which is clearly present, as discussed above.

The spectral energy distribution of IRAS 1652+395 is shown in Figure 6. It is evident from the figure that the *IRAS* power law (∼ −1.2), when extrapolated to X-ray wavelengths, predicts the measured *EXOSAT* flux well. The smooth curve is a simple fit given by the sum of a power law with a −1.2 slope and a standard galaxy spectrum. At 5400 Å, the 0.4 mJy of starlight is nearly half of the total (large-aperture) flux. Nonetheless, half of this is extended; starlight appears to produce only a little more than a quarter of the "nuclear" (i.e., unresolved) flux. There is marginal evidence for a small flattening of the power-law slope at wavelengths greater than 25 μm, which we describe here as $\Delta\alpha = 0.5$, as in Band and Malkan (1989).

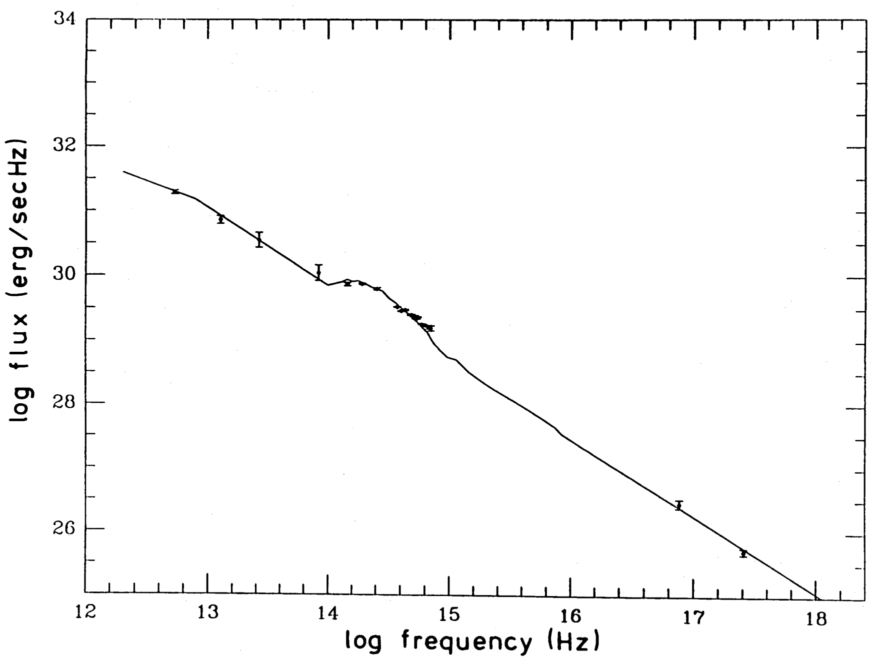

FIG. 6.—Spectral energy distribution of the new Seyfert galaxy, IRAS 1652+395. The smooth curve is a fit given by the sum of a power law of index $\alpha = -1.2$ and a standard galaxy spectrum.

Like many of the less luminous Seyfert 1 galaxies analyzed by Edelson and Malkan (1986), IRAS 1652+395 shows hardly any indication of any excess flux in the blue above this power law. The bluest optical point, at 4500 Å, might fall slightly above our starlight + power-law fit, but this excess is weaker than any "blue bump" detected by Edelson and Malkan (1986). To our knowledge, no "blue bump" has yet been detected in any narrow-line Seyfert 1 galaxy, and our observations of 1652+395 are consistent with this generalization.

IV. CONCLUSIONS

IRAS 1652+395 is a new Seyfert 1 galaxy with a redshift $z = 0.069$. Its optical spectrum is similar to the spectra of narrow-line Seyfert 1 galaxies (Osterbrock and Pogge 1985). The continuum from X-rays to far-infrared is typical of a moderately reddened active nucleus; an estimate of the internal reddening based on the Balmer decrement implies $E(B-V) < 0.2$. The object is the first previously unidentified AGN to be selected independently through its infrared and X-ray emission, and many more such objects may be found through future infrared and X-ray surveys.

We thank the Service observers at UKIRT and INT, Professor Barbieri and S. Unger for providing the exact position of the likely counterparts of the *IRAS* source and some of the VLA data respectively and to J. B. Stephen and E. Caroli for much help in the *EXOSAT* data reduction. The technical staff at the Lick Observatory, particularly R. Stone, and at the TIRGO Observatory helped with some of the optical and near-IR observations. Help from K. Byard in the taking and analysis of the *IUE* data is appreciated. The CCD detectors at Lick Observatory were developed with support from National Science Foundation grant AST 86-14510. We thank Wei-Hsin Sun and Wayne Webb for obtaining some of the 40 inch (1 m) Lick spectra. R. B. P. was supported in part by Grant N.AST-8616765 from the US National Science Foundation. L. S. acknowledges the receipt of a NATO-CNR Fellowship and was partly supported by the University of California at Los Angeles.

REFERENCES

Band, D. L., and Malkan, M. A. 1989, *Ap. J.*, in press.
Bassani, L., Caroli, E., Di Cocco, G., and Stephen, J. B. 1987*a*, Institute TE.S.R.E. Internal Report No. 123.
Bassani, L., Caroli, E., Stephen, J. B., and Di Cocco, G. 1987*b*, *IAU Circ.*, No. 4839.
Bassani, L., Coe, M. J., Mandolesi, N., Partridge, B., and Spinoglio, L. 1986, *Proc. of ESA Workshop on Space Borne Submm Astronomy Mission*, (ESA SP-260), ed. N. Longdon (Noordwijk: ESA), p. 151.
Bedford, D. K., Vilhu, O., and Petrov, P. 1988, *M.N.R.A.S.*, **234**, 319.
Burstein, D., and Heiles, C. 1978, *Ap. J.*, **225**, 40.
de Grijp, M. H. K., Miley, G. K., Lub, J., and de Jong, T. 1985, *Nature*, **314**, 240.
de Jong, Y., Klein, U., Wielebinski, R., and Wunderlich, E. 1985, *Astr. Ap.*, **147**, L6.
Edelson, R. A., and Malkan, M. A. 1986, *Ap. J.*, **308**, 59.
Edelson, R. A., Malkan, M. A., and Rieke, G. 1987, *Ap. J.*, **321**, 233.
Gaskell, C. M., and Ferland, G. J. 1984, *Pub. A.S.P.*, **96**, 393.
Heiles, C. 1975, *Astr. Ap. Suppl.*, **20**, 37.
Kriss, G. A., and Canizares, C. R. 1982, *Ap. J.*, **261**, 51.
Lauer, T. R., Miller, J. S., Osborne, C. S., Robinson, L. B., and Stover, R. J. 1984, in *Instrumentation in Astronomy V*. ed. D. L. Crawford, *Proc. SPIE*, Vol. **445**, p. 132.
Malkan, M. A. 1984, in *Proc. Garching Conference on X-ray and UV Emission from Active Galactic Nuclei*, ed. W. Brinkman and J. Trumper (Garching: MPE Report 184), (Max-Planck Institut), p. 21.
Malkan, M. A., and Sargent, W. L. W. 1982, *Ap. J.*, **254**, 22.
Margon, B., Chanan, G. A., and Downes, R. A. 1982, *Ap. J.* (*Letters*), **253**, L7.
McLean, I. S., Chuter, T. C., McCoughrean, M. T., and Ryner, J. T. 1986, in *Instrumentation in Astronomy VI*, ed. D. L. Crawford, *Proc. SPIE*, Vol. **627**, p. 430.
Miley, G. K., Neugebauer, G., and Soifer, B. T. 1985, *Ap. J.* (*Letters*), **293**, L11.
Osterbrock, D. E. 1977, *Ap. J.*, **215**, 733.

Osterbrock, D. E., and Pogge, R. W. 1985, *Ap. J.*, **297**, 166.
Reichert, G. A., Mason, K. O., Torstensen, J. R., and Bowyer, S. 1982, *Ap. J.*, **260**, 437.
Stone, R. P. S. 1974, *Ap. J.*, **193**, 135.
———. 1977, *Ap. J.*, **218**, 767.
Thompson, A. R., Clark, B. G., Wade, C. M., and Napier, P. J. 1980, *Ap. J. Suppl.*, **44**, 151.
Ward, M., Elvis, M., Fabbiano, G., Carlton, N. P., Willner, S. P., and Lawrence, A. 1987, *Ap. J.*, **315**, 74.

L. Bassani and N. Mandolesi: Istituto TE.S.R.E. (C.N.R.), Via De' Castagnoli 1, 40126 Bologna, Italy

M. J. Coe: Physics Department, Southampton University, Highfield, Southampton, SO9-5NH, United Kingdom

M. N. Malkan: Astronomy Department, University of California, Los Angeles, CA 90024

B. Partridge: Astronomy Department, Haverford College, Haverford, PA 19041

L. Spinoglio: Istituto F.S.I. (C.N.R.), Casella postale 27, 00044 Frascati, Italy